Proposal of a Photosensor Circuit for Point-Of-Care Optical Immunoassay

YuTong Zhang

October 5th, 2015

BIOE 385

Dr. Ramos

I. Executive Summary

Point-of-care diagnostic systems are critical for providing affordable, effective and time conscientious treatment for patients in developing countries. One of the main areas that needs to be developed is blood analysis. Current methods require lengthy sample purification, incubation and rinsing steps before analysis can take place. Thus, we aim to engineer a rapid, accurate, precise and cost-effective whole blood analytical tool for use on patients in low-income or underdeveloped regions.

Our team has designed an optical immunoassay consisting of a LED/photodiode hardware system and a data analyzing LABview software system to measure for whole blood nanoshell conjugated particulates. This system can then output concentrations and percentages of the nanoshell aggregates which can then be translated to a diagnosis. We investigated two different approaches to creating a photodiode circuit. One utilized a photoconductive set up while the other used a photovoltaic set up.

After extensive testing and evaluation of project constraints, we recommend the photovoltaic circuit to be implemented for optical immunoassay measurements. This circuit gives very precise and accurate measurements as well as is easy to implement. It also is more cost efficient which is more suitable for our targeted customers. In this paper, I will detail the goals and methods, circuitry, LABview program, and testing results of our device in order to justify our recommendations.

With its accurate and precise measurements of nanoshell aggregates in whole blood as well as the clear relationship established between nanoshell aggregation and particulates present that can be used for easy diagnosis, our product would allow for better and more efficient care for patients in the developing world.

II. Introduction

A great number of nations on the modern day map still fall under the "developing" category. Patients in these countries receive substandard care because of a lack of resources, lack of time as well as lack of technologies adapted for challenges of that setting. Especially in regards to blood testing, current methods are long and tedious as well as requires a great deal of equipment, time and money. This prompts a need for a blood analysis device that can be cost effective, user friendly, easy to implement, accurate and precise.

Our goal is to create such a device through the use of an optical immunoassay system. Blood analysis via optical immunoassay measurements is accomplished by allowing nanoshell conjugated antibodies to bind for the specific particulates in question. These nanoshells will then aggregate to form structures that attenuate the light that can be passed through to the photodiode. Since there is a direct relationship between the amount of aggregation and light attenuation, measurements of the changes in light can yield concentration values. To make an even simpler device than the traditional optical immunoassays, we will be utilizing light source of only one wavelength and thus omitting the need for complicated parts such as a spectrophotometer. Our approach begins with building the appropriate hardware such as the LED circuits and the photodetector circuits on protoboards with slots for test samples. Once reasonable values were procured from those circuits, a LABview program was constructed as an interface to receive voltage signals, perform automatic calibrations, display various percentages and concentrations as well as save data in the display table and excel.

III. LED Circuits

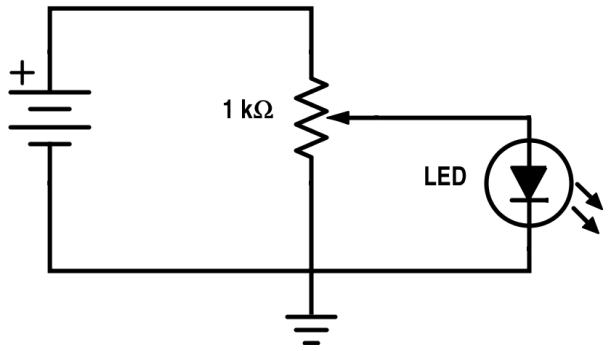

Figure 1: LED circuit

A LED circuit was constructed with an 850 nm 530E850C LED, a 1000 Ω potentiometer and a 5 V DC power source. An 850 nm LED was chosen because the specific type of nanoshells used attenuates the most light with that wavelength which give us better accuracy and a more drastic range to work with[1]. The potentiometer was able to regulate the amount voltage delivered to the LEDs so that it did not exceed its accepted range of 1.5 V – 1.8 V. The voltage across the LEDs was maintained at 1.349 V and 1.435 V for the photovoltaic and photoconductive circuits respectively. This ensures that the LED will not have a surplus of current that will cause it to blow up or a lack of current that will result in an unlit LED.

IV. Photoconductive Circuit

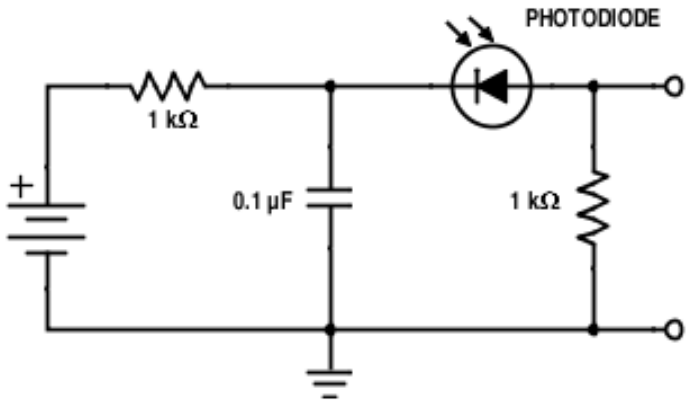

Figure 2: Photoconductive circuit

In this circuit, a FDS100 photodetector is powered by a DC voltage of 5 V and is connected with an RC circuit as well as a load resistor. This RC circuit behaves as a low pass filter because the time it takes for the capacitor to charge up increases as frequency increases. The relationship between the capacitor delay and its filter effects can be visualized with the following equation:

$$V_{out} = V_{in} \frac{1}{\sqrt{1 + \omega^2 R^2 C^2}}$$

This equation can be derived by calculating for circuit impedance and finding the ratio of V_{in} to V_{out}. This equation demonstrates that as frequency increases, the transfer function will approach 0. This results in the attenuation of the signals at frequencies higher than the cutoff frequency created by the combination of resistor and capacitor values used. The values chosen for this RC circuit were respectively 1000 Ω and 0.1 µF for the resistor and capacitor. This gave us a cutoff frequency of 1591.6 Hz when the following equation was utilized:

$$f_c = \frac{1}{2\pi RC}$$

These values were chosen because they were recommended by the photodiode data sheet to filter out any intrinsic noise the photodiode was generating. This circuit is driven by a voltage input that increases its speed of response. This input voltage is able to increase the width of the photodiode's depletion layer which leads to faster response due to a decrease in junction capacitance[2]. Lower capacitance means lower charge up time. Although this gives a faster response, it also induces a much larger dark current. The voltage difference applied to the photodiode to cause a faster response actually causes a dark current. This increase in dark current actually generates a lot of noise and detracts from the accuracy of this photosensor. This circuit also includes a load resistor which can amplify output voltage of this circuit as resistance values increase. We chose a value of 1000 Ω for R_{LOAD} because it gave us voltage values that allowed us to maximize usage of our full available voltage. However, a complication of using a large resistor to amplify the voltage is that as the resistor values increase, so does the noise it generates.

V. Photovoltaic Circuit

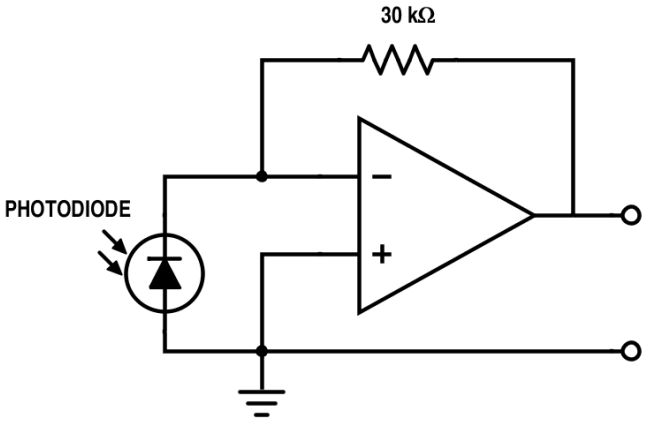

Figure 3: Photovoltaic circuit

This photovoltaic utilizes an OP07op-amp to amplify the voltage of the photodetector. The op-amp is powered by a DC voltage of ±15 V and has an inverting set

up with the ground connected to the + end. It detects and amplifies the voltage difference between the – and + terminals. A negative feedback resistor of 30 kΩ was placed from the output voltage branch to the negative input. This allows for the output voltage to regulate the amount of amplification that occurs. This relationship can be characterized by the following transfer function:

$$\frac{V_{out}}{V_{in}} = -\frac{R_F}{R_{Photodiode}}$$

There exists a direct relationship between R_F and the output voltage. A derivation of this transfer function can be obtained to better describe the relationship between the current generated by the photodiode and the feedback resistor:

$$V_{out} = -I_{Photodiode}R_F$$

After trial and error, we found that 30 kΩ gave us the best output voltage that was large enough to be accurate and detectable but small enough to not turn the op-amp into a comparator and cause constant max voltage output[3].

The photovoltaic circuit is able to minimize the production of a dark current because there is mostly no voltage difference across the photodiode. This allows for a reduction in noise otherwise caused by the presence of a dark current giving this circuit better theoretical precision. However, it will have slower response times than those of the photodiode in the photoconductive circuit. In addition, any noise received through the photodiode will simply be uniformly amplified with op-amp.

VI. LABview Program

a. Data Acquisition and Processing

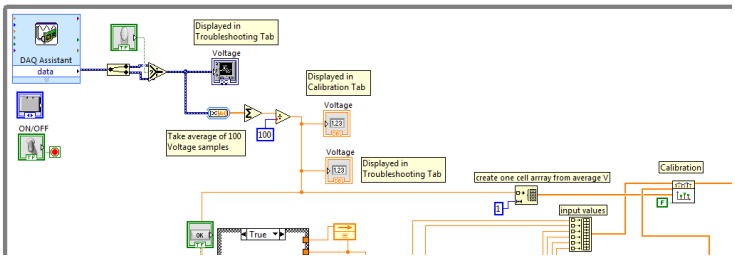

Figure 8: Block Diagram – Acquisition and Signal Averaging

Our program is situated within a while loop that is continuously running as long as the power toggle on the front panel is switched to 'ON'. Voltage signals from both photovoltaic and photoconductive circuits are acquired through a DAQ assistant simultaneously. These two signals are sent to a boolean signal selector which depending on the true/false signal it receives from a button on the front panel, will select either the photoconductive circuit output voltage or photovoltaic circuit output voltage. This feature allows for the program to switch seamlessly from one circuit to the other. Once a signal is selected, it is changed from dynamic data to a data array. By using not every single of the 100 samples but an average of them, we can attain better stabilization of the processed values and representation of all the samples. This was done by summing up the array of values and dividing by 100. By average each set of 100 samples, we were able to procure more consistent and accurate values. These values are then sent to the calibration section or displayed accordingly.

b. Calibration

Figure 4: Front Panel – Calibration Tab

This is the calibration section of our program's front panel. On this tab, there includes instructions on how to calibrate the system and 6 calibration slots. In these slots, percentages of the calibration samples can be inputted and once the 'calibrate' button is pressed, the corresponding voltage values are recorded and processed within the program.

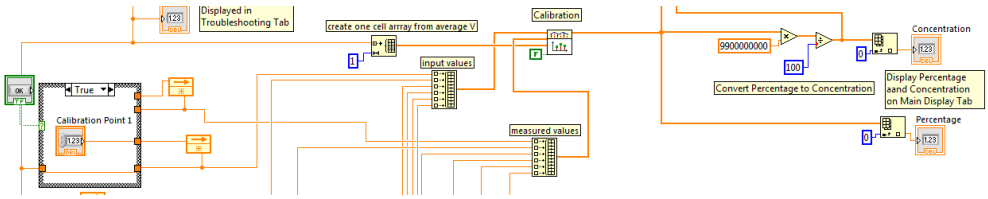

Figure 5: Block Diagram – Calibration

Once the percentage inputs and the recorded voltages are obtained, they will both be fed into a case structure. There are a total of 6 identical case structures that process each individual pair of voltages and percentages. These case structures are all linked to their individual 'calibrate' button on the front panel. Once clicked, each case structure will be briefly true and will fetch both the inputted percentage as well as the measured voltage value at that instant. When the case structure is false again, these two values will be outputted into an array. This array will be given to the interpolation subVI which will

allow for calibration to take place automatically. The subVI will also have an input of the voltage for unknown percentages that we are trying to test. The interpolation subVI will use linear interpolation which essentially means constructing a linear relationship line between each of the inputted array points. From the constructed interpolation lines, it is able to find the corresponding percentage for the given measured voltage.

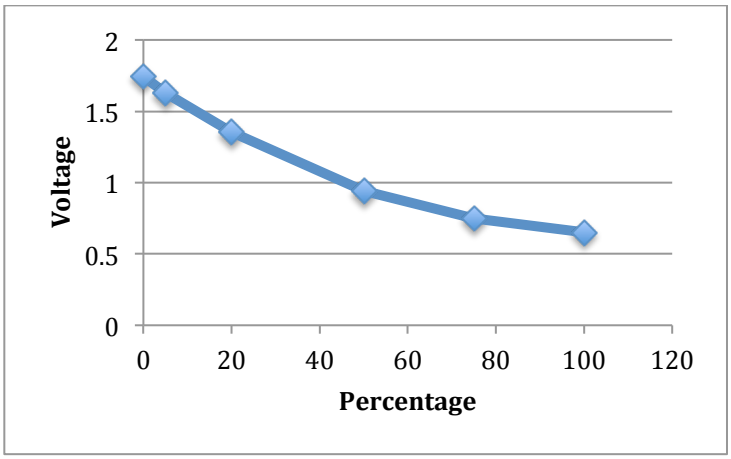

Figure 6: Calibration Values for Photoconductive Circuit with Linear Interpolation Lines

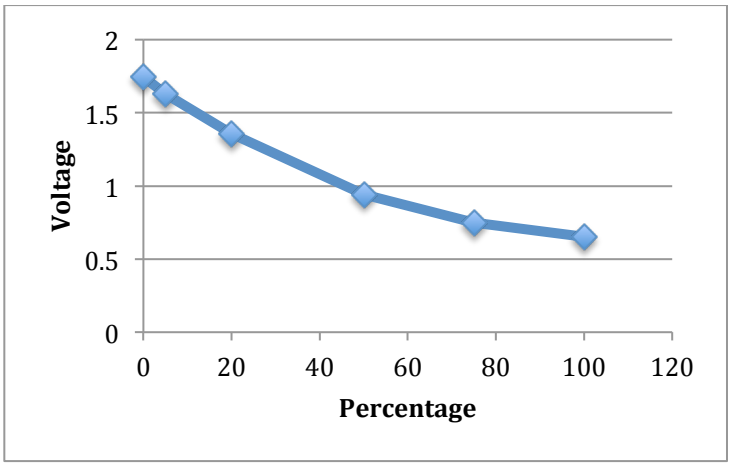

Figure 7: Calibration Values for Photovoltaic Circuit with Linear Interpolation Lines

c. Table Building and Data Saving

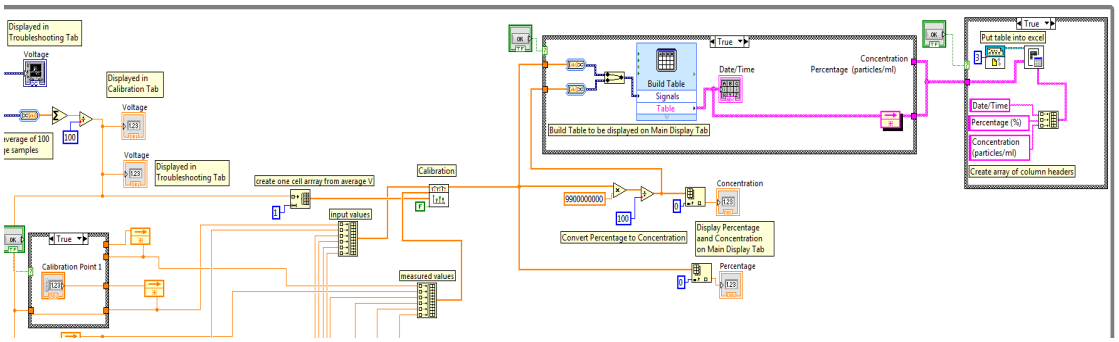

Figure 9: Block Diagram – Table Display and Data Saving

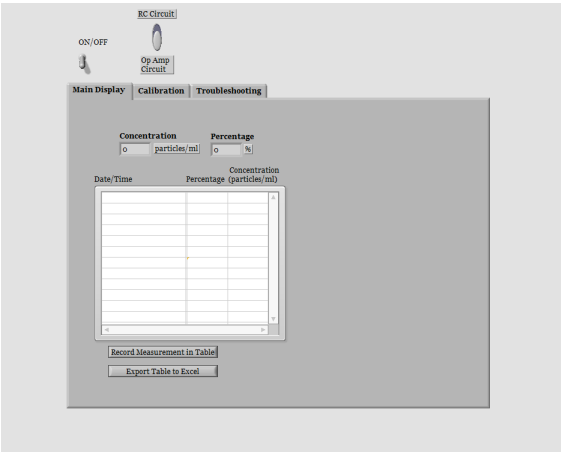

Figure 10: Front Panel – Main Display Tab

As detailed in the section above, the interpolation subVI is able to output a percentage for any given voltage based on the initial calibration values. The output of this subVI will then be multiplied by the maximum concentration to get the corresponding concentrations. These concentrations along with its percentage can then be saved in a table by utilizing a case structure. Although the instrument is constantly measuring for and displaying voltages and their corresponding percentages, it is desirable that specific values can be recorded in an easy to read format on the front panel. Once the user is ready to record a value, they can simply hit the "Record Measurement in Table' button to activate the case structure that contains the build table subVI. Within this case structure,

is a build table subVI which can take the input concentrations and percentages and display them on the front panel in form of a table. Once the desired concentrations and percentages are saved into a table, the user may want to export these values to some easily savable medium such as excel. In order to do so, our program incorporated another case structure. This case structure only accepts the output of the table case structure and thus, saves only the values within the table. It is able to build a report, which is then sent to the put table in excel subVI along with the table values obtained in the previous case structure. This allows for the user to save the data they have collected in form of an excel spreadsheet.

VII. Testing and Results

These completed circuits were intensively tested to determine which one would have better accuracy and precision. It is critical that a designed blood analytical assay has both so it can both correctly as well as repeatedly detect for targeted particulates. Values were gathered through five trials. Each trial tested six known percentages to generate a total of thirty interpolated percentages for analysis. The measured percentages were then compared to the actual percentages. In order to investigate accuracy, I looked at the percent differences between the mean difference and the actual percentage values. This can quantitatively describe the proximity of measured values to actual values, which will give a good characterization of the device's accuracy. Percent difference was not calculated for 0 because the formula used would yield an undefined answer:

$$Percent\ Differnce = \frac{Test\ Value - Mean\ Difference}{Test\ Value} \times 100$$

For the photoconductive circuit, the percent differences fluctuated as well as had a range extending to past 6% for some test values. A percent difference of 6% would be able to

change the concentration $\pm$ 5.94 x 10^6 particles/mL per measurement. This could potentially cause mistakes with diagnosis because of the noticable deviation from the actual values.

Precision was also measured to ensure that values were consistent over time. Since precision is characterized by reproducibility and repeatability, we can determine it by simply analyzing the data set for the standard deviations. Determining the standard deviation of a data set allows for quantification of the amount of variation or dispersion within it. The same data used for accuracy were repeated for precision analysis. These data values and the following equation were used to calculate for the standard deviations:

$$Standard\ Deviation = \sqrt{\frac{\Sigma\ (\text{trial} - \text{mean})^2}{\#of\ samples - 1}}$$

The standard deviations of these trials for each test values were also varied ranging from 0.2 deviations to almost 2 deviations away. The standard deviation values were generally close to a whole deviation away from the mean.

Actual Values	Trial 1	Trial 2	Trial 3	Trial 4	Trial 5
0	-0.98	-1.36	-0.15	1.23	0.24
5	4.32	4.25	4.51	5.98	4.35
20	20.7	20.66	20.55	20.85	22.76
50	50.051	51.74	50.01	50.68	50.72
75	75.22	75.32	75.33	75.34	75.89
100	101.98	100.75	102.38	104.45	105.03

Figure 11: Data Table for Photoconductive Circuit Measured Values

Actual Values	Mean Difference	% Difference	Std Dev
0	-0.204	-	1.024
5	4.682	6.36	0.732
20	21.104	-5.52	0.932
50	50.64	-1.28	0.700
75	75.42	-0.56	0.267
100	102.92	-2.92	1.780

Figure 12: Statistical Analysis for Photoconductive Circuit

For the most accurate as well as precise data values, the trend line should have an equation of $y = x$. This indicates the measured values are exactly the same as the actual values. The linear regression equation obtained for the plot of all thirty-five collected values was $y = 1.0228x + 0.1918$. The coefficient is close to one and the intercept is near zero. The linear regression fits well with the data values with an R^2 value of 0.9991. This is a good linear regression equation that indicates good accuracy and precision for this circuit.

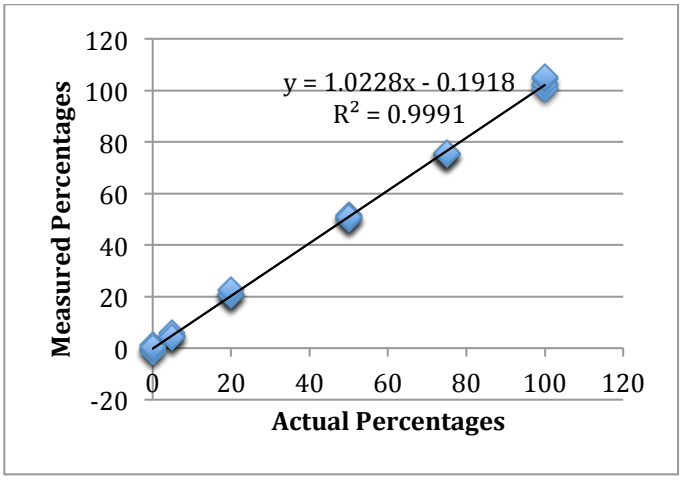

Figure 13: Graph for Photoconductive Circuit - Measured v. Actual

The photovoltaic circuit was subjected to the same amount and kind of testing. Five trials were run and thirty total values were obtained. Accuracy of the circuit was determined by calculating for percent differences in the measured values versus the actual values. The resulting percent differences had some variation with the range extending past 1%.

Precision was again assessed by calculating for the standard deviation of the data sets. The resulting standard deviations were all under one deviation away from the mean and very small. The variation is fairly small within the different standard deviation values.

Actual Values	Trial 1	Trial 2	Trial 3	Trial 4	Trial 5
0	0.49	-0.19	-0.07	0.21	-0.14
5	5.1	4.94	5.04	4.93	4.65
20	19.88	19.89	20.17	20.95	19.98
50	49.92	49.96	49.98	50.33	49.84
75	74.76	74.97	74.94	74.95	74.47
100	99.89	99.87	99.92	99.97	99.57

Figure 14: Data Table for Photovoltaic Circuit Measured Values

Actual Values	Mean Difference	% Difference	Std Dev
0	0.06	-	0.286
5	4.932	1.36	0.173
20	20.174	-0.87	0.449
50	50.006	-0.012	0.189
75	74.818	0.243	0.212
100	99.844	0.156	0.158

Figure 15: Statistical Analysis for Photovoltaic Circuit

Once again the desired regression line would have the format of $y = x$. This assumes a perfect correlation between actual percentages and measured percentages. When the data values were graphed and the linear regression line was $y = 0.9977x + 0.0691$. The coefficient is almost one and the intercept is almost zero. It was also shown that the linear regression fit very well to the data values with an R^2 value of 0.99995. This is a very favorable linear regression equation that demonstrated good accuracy and precision for this circuit.

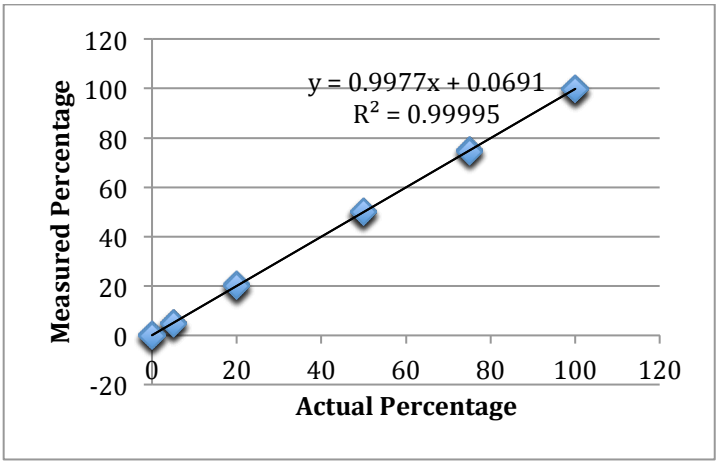

Figure 16: Graph for Photovoltaic Circuit - Measured v. Actual

After collection of data for both circuits, a comparison must be made in order to determine the circuit with more accuracy and precision. The better circuit was determined by comparing the average percent difference, average standard deviation and trend line coefficients and intercepts. The photovoltaic circuit had lower average percent difference as well as standard deviation. This indicates better accuracy for the photovoltaic circuit for future interpolations of percentages since the accuracy for the calibration values determine its functionality when it comes to unknown percentages. In addition, a linear regression fit better for the data values obtained with the photovoltaic circuit with a higher R^2 value. Lastly, the linear regression line of the photovoltaic circuit has a coefficient that deviated from the ideal coefficient of one as much as the photoconductive linear regression coefficient. However, its intercept was closer to zero than the photoconductive linear regression intercept by a significant amount. A more ideal linear regression fit indicates both better precision and accuracy. Values with a near ideal linear regression demonstrate small deviations from actual values and less measured value variation.

Circuit Type	Average % Difference	Average Std. Dev.	R^2	Regression Coefficient	Regression Intercept
Photoconductive Circuit	-0.784	0.906	.9991	1.023	0.192
Photovoltaic Circuit	0.175	0.244	.9999	0.977	0.0691

Figure 17: Statistical Comparison of Photovoltaic and Photoconductive Circuits

VIII. Recommendation

a. Accuracy and Precision

After testing and statistical analysis, the photovoltaic circuit demonstrated better accuracy and precision than the photoconductive circuit with smaller percent differences, smaller standard deviations as well as a more ideal linear regression line.

b. Cost

Component	Cost ($)
530E850C LED	0.19[1]
2 x 1 kΩ Resistor	0.36[2]
1 kΩ Potentiometer	8.58[3]
0.1 μF Capacitor	1.25[4]
FDS100 Photodiode	13.50[5]
Total:	23.88

Figure 18: Cost of Photoconductive Circuit

[1] http://www.electron.com/led-5mm-infrared-ir-530e850c.html
[2] http://www.amazon.com/E-Projects-Ohm-Resistors-Watt-Pieces/dp/B00B5R8950
[3] http://www.amazon.com/Gikfun-3296W-102-Trimmer-Potentiometer-Arduino/dp/B00UAFQIDI/ref=sr_1_1?s=pc&ie=UTF8&qid=1443938626&sr=1-1&keywords=1k+ohm+potentiometer
[4] http://comingsoon.radioshack.com/0-1uf-50v-hi-q-ceramic-disc-capacitor-pk-2/2720135.html
[5] http://www.thorlabs.com/thorproduct.cfm?partnumber=FDS100

Component	Cost ($)
530E850C LED	0.19[6]
OP07 Op-Amp	0.11[7]
30 kΩ Resistor	0.10[8]
1 kΩ Potentiometer	8.58[9]
FDS100 Photodiode	13.50[10]
Total:	22.48

Figure 19: Cost of Photovoltaic Circuit

The total cost of a constructing a photovoltaic circuit is $22.48 while the total cost for a photoconductive circuit is $23.88. A photovoltaic circuit is $1.40 cheaper than a photoconductive, which makes it the more cost effective circuit. Since our targeted audience resides in developing areas, maintaining a low cost device is very important. Thus, the photovoltaic circuit better suits the cost effective aspect of our goal.

c. Ease of Implementation

The photoconductive circuit requires six components to construct while the photovoltaic circuit requires only five. The photovoltaic circuit is also a much simpler design requiring less connections and wiring which ultimately allows less room for error. They both require structure to keep the samples steady and ensure consistent placement. The space they occupy is very similar and one has no significant advantage over the other. Overall the ease of implementation is comparable between the two circuits with the photovoltaic circuit having a slight simpler set of components to work with and set up.

---

[6] http://www.electron.com/led-5mm-infrared-ir-530e850c.html
[7] http://www.tme.eu/en/details/op07cp/tht-operational-amplifiers/texas-instruments/?brutto=pl&currency=USD&gclid=Cj0KEQjw-b2wBRDcrKerwe-S5c4BEiQABprW-JF48YdHEDnO8D7OmFHjgocncgGgZyqmj5GdFPF5ZuoaAm3L8P8HAQ
[8] http://www.digikey.com/product-detail/en/CFR-25JB-52-30K/30KQBK-ND/1525
[9] http://www.amazon.com/Gikfun-3296W-102-Trimmer-Potentiometer-Arduino/dp/B00UAFQIDI/ref=sr_1_1?s=pc&ie=UTF8&qid=1443938626&sr=1-1&keywords=1k+ohm+potentiometer
[10] http://www.thorlabs.com/thorproduct.cfm?partnumber=FDS100

d. Recommended Circuit

Ultimately, considering the accuracy and precision, cost and ease of implementation of the two different circuit designs, our team has decided to recommend the photovoltaic circuit for the final design of this optical immunoassay. Based on its superior accuracy and precision as decided by statistical factors, lower costs and slightly easier implementation, it will be the best circuit to provide an exact blood analytical tool that fits the parameters developed for the target setting of developing areas.

Parameters	Photoconductive	Photovoltaic
Accuracy		✓
Precision		✓
Cost		✓
East of Implementation		✓

Figure 20: Comparison of Parameters met by Photoconductive and Photovoltaic Circuits

e. Limitations and Design Expansions

One of the limitations of our design is a purely structural one. In order for accurate and precise percentages to be measured, the blood sample but be placed in the exact same spot each time both during actual testing and calibration. However, our structures composed of paper and tape were at times too flimsy to be the kind of secure and consistent structure that would be ideal for our device. This limited the accuracy and precision we were able to obtain for the photovoltaic circuit. In the future, this structure will certainly be replaced with more durable and sturdy materials as the design of this optical immunoassay proceeds forward.

Another limitation is the variable noise that can be generated based on the surroundings of the circuitry due to a lack of isolation of the circuit from its environment. We did not have proper structures built around the circuitry to prevent any fluctuations in

the device surroundings from affecting its accuracy and precision. This can be adjusted by building isolation chambers for the circuit to ensure that the LED is responsible for the only light variable.

The signals acquired by the photovoltaic circuit are still not completely free of noise. By addressing this issue, the accuracy and precision for the photovoltaic circuit could be even better. The photovoltaic circuit utilizes an op-amp to amplify the entirety of the signal, which results in all of the noise in the signal also being amplified. Both of these circuits could benefit from selective filters being implemented to attenuate unwanted signals at certain frequencies. In the future, filters should be implemented and tested to help generate cleaner, better signals.

Lastly, to truly have a firm determination of good accuracy and precision, a wider range of samples must be utilized for testing. We were only able to test six values during the construction of the circuit as well as the final determination test for the better circuit. This could be a limitation since it gives us measured percentages for our calibration values, which could give an incomplete picture of the overall function of the detection system. As this device proceeds forward in design and production, a wide and diverse selection of samples must be used to better assess accuracy and precision.

IX. Conclusion

Through the extensive testing and data analysis of these two circuits, our team was able to come to a

recommendation of the photovoltaic circuit for the final design of the optical immunoassay device. Despite the two circuits being both very effective at nanoshell aggregate detection, the photovoltaic circuit was superior with better accuracy and precision, lower costs, and easier implementation. Although there are certainly improvements and modifications that can be made going forward such as structural changes, more extensive filtering as well as better testing, this circuit has demonstrated proficiency as an optical detector for an accurate, precise, cost-effective, and easy to use point-of-care whole blood analyte detection device.

References

1. Hirsch, L. R., J. B. Jackson, A. Lee, N. J. Halas, and J. L. West. "A Whole Blood Immunoassay Using Gold Nanoshells." *Analytical Chemistry* 75.10 (2003): 2377-381. Print.

2. Scherz, Paul, and Simon Monk. *Practical Electronics for Inventors*. 1st ed. Mcgraw-Hill Education, 2000. 204. Print.

3. Scherz, Paul, and Simon Monk. *Practical Electronics for Inventors*. 1st ed. Mcgraw-Hill Education, 2000. 204. Print.